Covalent versus localized nature of 4f electrons in ceria: Resonant angle-resolved photoemission spectroscopy and density functional theory

Tomáš Duchoň,[1,*] Marie Aulická,[1] Eike F. Schwier,[2] Hideaki Iwasawa,[2] Chuanlin Zhao,[3] Ye Xu,[3,†] Kateřina Veltruská,[1] Kenya Shimada,[2,‡] and Vladimír Matolín[1,§]

[1]*Faculty of Mathematics and Physics, Charles University, V Holešovičkách 2, 18000 Prague 8, Czech Republic*
[2]*Hiroshima Synchrotron Radiation Center, Hiroshima University, Higashi-Hiroshima, Hiroshima 839-0046, Japan*
[3]*Department of Chemical Engineering, Louisiana State University, Baton Rouge, Louisiana 70803, USA*

(Received 31 January 2017; published 18 April 2017)

We have conducted resonant angle-resolved photoemission spectroscopy of well-defined $CeO_2(111)$ and c–$Ce_2O_3(111)$ model surfaces, revealing distinct f contributions in the valence band of the two compounds. In conjunction with density functional theory calculations, we show that the f contribution in CeO_2 is of a covalent nature, arising from hybridization with the O 2p bands. In contrast, c–Ce_2O_3 exhibits an almost nondispersive f state at 1.3 eV, which is indicative of almost negligible c-f hybridization.

DOI: 10.1103/PhysRevB.95.165124

I. INTRODUCTION

The ground state of CeO_2 has been a controversial topic [1–10]. The controversy involves the assignment of the nominally ionic CeO_2 as either a mixed valent or a covalent compound, and it arises partially due to the inability to distinguish these electronic configurations using core-level photoelectron spectroscopy, namely that of the Ce 3d level [10]. Strikingly, the ambiguity of the assignment is still prevalent in the scientific literature [11], sustained by a loose usage of the respective terms. By definition, mixed valent compounds contain cations in different oxidation states. The distinguishability of crystal sites occupied by the cations is related to the extent of the mixing between the configurations (typically cation-cation mixing) [12]. This effectively leads to either a highly unusual integral or nonintegral mean oxidation state of the cation [13]. On the other hand, covalent compounds contain only one type of cation site, and they exhibit a nonintegral valence as a consequence of hybridization (typically cation-anion mixing) [14]. In the case of ceria, where there are no crystallographically distinguishable cerium sites in the lattice, the fundamental difference between the two configurations lies in the character of the occupied states. The homogeneous mixed valent ground state would feature a partial occupation of the highly localized atomiclike Ce 4f level [15] through valence fluctuation, while the covalent ground state would exhibit an empty Ce 4f level with the bonding electrons spin-paired with the ligand (specifically the closed O 2p shell) [14]. The two configurations would manifest different responses to electronic perturbations, such as a core hole, an oxygen vacancy, foreign interstitial or substitutional species, adsorbates, or electronic potential in an electrochemical device. The importance of understanding the behavior of the electrons in ceria due to said perturbations is highlighted by recent studies showing gaps in understanding the bonding mechanism and reactivity of ceria [16] and metal oxides in general [17].

Notably, the established mixed valent interpretation of core-level photoemission from ceria [1], based on the semiempirical Gunnarson-Schönhammer theory utilizing a single-impurity Anderson Hamiltonian, has been called into question. Rigorously calculated configuration interaction wave functions for CeO_2 and Ce_2O_3 were used to provide an *ab initio* theoretical description of core-level photoemission accounting for many-body effects [18–20]. The results show that experimental spectra can be modeled through covalent interaction, revealing possible errors in the former approach.

Motivated by the above-mentioned controversy and the unsatisfactory understanding of photoemission in ceria in general, herein we present the results of a combined angle-resolved photoemission spectroscopy (ARPES) and density functional theory (DFT) study of the 4f electrons in ceria. Leveraging recent advances in *in situ* preparation of well-defined ceria model surfaces, we directly compare CeO_2, a nominal 4f^0 compound, and c–Ce_2O_3, a nominal 4f^1 compound, and we reveal the covalent nature of the 4f admixture into the O 2p valence band in CeO_2 in contrast to the highly localized 4f electrons in c–Ce_2O_3. As a consequence, we show that the resonant photoemission enhancement at the $4d \rightarrow 4f$ absorption threshold in CeO_2 does not originate from the occupation of localized 4f states on Ce atoms in the ground state, rather it arises from the covalent character of the O 2p valence band through interatomic effects.

II. METHODS

ARPES measurements were performed with 110–130 eV p-polarized photons on the linear undulator beamline BL-1 at the Hiroshima Synchrotron Radiation Center (HiSOR) at Hiroshima University. The energy and momentum resolution were set at 30 meV and 0.015 $Å^{-1}$, respectively. The experiments were carried out with the sample cooled down to 12 K. Highly ordered epitaxial ceria films exposing the (111) surface of the fluorite lattice were prepared by reactive evaporation of Ce onto Cu(111) single crystal in 5×10^{-5} Pa of O_2 at a substrate temperature of 250 °C in the preparation chamber connected to the ARPES chamber. The films were around 3 nm thick, which is thick enough to guarantee continuity and mitigation of possible size effects [8,21] while still being

*Corresponding author: aritentd@gmail.com
†yexu@lsu.edu
‡kshimada@hiroshima-u.ac.jp
§matolin@mbox.troja.mff.cuni.cz

thin enough to avoid charging during measurements. The stoichiometry of the prepared layers was carefully controlled using a Ce-ceria interfacial reaction [22]. The preparation procedure has been described in detail in Ref. [21]. Briefly, metallic Ce is deposited onto a ceria surface and the sample is heated to 600 °C. The elevated temperature allows oxygen to diffuse through the ceria lattice to the Ce metal overlayer, which then oxidizes and adopts the fluorite structure of the underlying ceria.

Spin-polarized DFT calculations based on the Heyd-Scuseria-Ernzerhof (HSE06) [23] hybrid functional were carried out using the projected augmented wave (PAW) method as implemented in VASP (version 5.3) [24,25]. The ($4f$,$5s$,$5p$,$5d$,$6s$) states of Ce and the ($2s$,$2p$) states of O were treated as valence states and expanded using a plane-wave basis set up to 400 eV. For bulk CeO_2, the lattice constant was optimized on an ($11\times11\times11$) Monkhorst-Pack k-point grid to be 5.40 Å, and the O $2p$-Ce $4f$ band gap was calculated to be 3.5 eV, both in close agreement with previous experimental (5.41 Å [26] and 3 eV [3]) and HSE06 results (5.41 Å and 3.3 eV [27]). The equilibrium lattice constant of c–Ce_2O_3 (bixbyite) was calculated to be 11.20 Å (versus the experimental value of 11.16 Å [28]) with all atoms in the bulk unit cell fully relaxed to below 0.03 eV/Å and the k-space sampled at the Γ point only. The antiferromagnetic state was used, although it was only marginally more stable than the ferromagnetic state. Electronic structures were calculated on a ($3\times3\times3$) Monkhorst-Pack k-point grid using the frozen optimized bulk structure. The Ce $4f$-$5d$ band gap was calculated to be 2.6 eV (versus the experimental value of 2.4 eV [29]). Core-level electron excitation ($4d \rightarrow 4f$) was done using the method of Köhler and Kresse [30] and was applied to all Ce atoms in CeO_2 and c–Ce_2O_3. The bulk oxidation energy for $c\text{–}Ce_2O_3 + \frac{1}{2}O_2 \rightarrow 2CeO_2$ was calculated to be -3.12 eV, with available estimates falling between -3.5 and -4.0 eV at ambient temperature [31,32].

III. RESULTS AND DISCUSSION

To elucidate the nature of the ground state of CeO_2, we use c–Ce_2O_3 as a reference $4f^1$ compound [22]. The advantage of this approach over other prototypical $4f^1$ compounds that have been previously used for the purpose, such as CeF_3 [5], is that it minimizes the influence of structural and chemical variation on the electronic configuration. The Ce sublattice in both CeO_2 and c–Ce_2O_3 is practically identical, the only difference being ordered oxygen vacancies in the O sublattice in c–Ce_2O_3 [33]. Moreover, we can exploit the isostructural $CeO_2 \leftrightarrow c\text{-}Ce_2O_3$ transition and use one sample for both systems, further reducing the extrinsic contributions to our experimental results [21].

Resonant photoemission is a commonly used tool for enhancing the intensity of photoemission features originating from states with low density and for gauging hybridization strength in correlated electron systems, especially the c-f hybridization of cerium compounds [34]. Particularly in ceria, the $4d \rightarrow 4f$ resonant transition is routinely used to reveal the occupation of the $4f$ state, a fingerprint of Ce^{3+} [35]. However, both CeO_2 and c–Ce_2O_3 exhibit a resonant enhancement at the $4d \rightarrow 4f$ photoabsorption threshold (125 and 121 eV

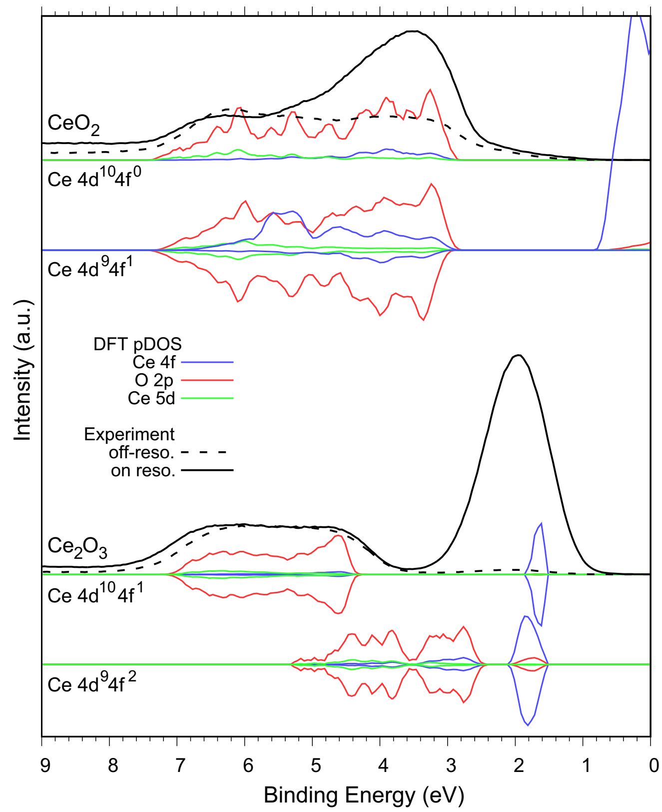

FIG. 1. Partial density of states (pDOS) of CeO_2 and c–Ce_2O_3 as calculated using the HSE06 exchange-correlation functional and measured by photoelectron spectroscopy (PES). The pDOS has been calculated for the ground state of CeO_2 and c–Ce_2O_3 and for an intermediate state with a Ce $4d$ electron excited into the Ce $4f$ level. The PES spectra are shown as measured off (dashed black lines, $h\nu = 115$ eV) and on (solid black lines, $h\nu = 125$ and 121 eV for CeO_2 and c–Ce_2O_3, respectively) the Ce $4d \rightarrow 4f$ resonance. The calculated DOS is shifted to coincide with the experimental data (the actual Fermi energy of the DOS plots in the figure is at 2.9 and 1.55 eV for CeO_2 and c–Ce_2O_3, respectively). The c–Ce_2O_3 pDOS has been scaled down by a factor of 32 to account for the higher number of Ce atoms in the unit cell in comparison with CeO_2.

for CeO_2 and c–Ce_2O_3, respectively), albeit with different characters. The resonant feature in c–Ce_2O_3 directly overlaps the direct photoemission $4f$ peak and has comparable width, while the resonant feature in CeO_2 overlaps the top of the O $2p$ band and is noticeably wider than the $4f$ photoemission peak in c–Ce_2O_3. The valence-band photoemission spectra showing the resonant enhancement at the $4d \rightarrow 4f$ photoabsorption threshold for CeO_2 and c–Ce_2O_3 are shown in Fig. 1.

The resonant enhancement in c–Ce_2O_3 can be explained by constructive interference of the direct photoemission from the $4f$ level with an indirect super Coster-Kronig decay of an intermediate $4d^9 4f^2$ state:

$$4d^{10}4f^1 + h\nu \rightarrow 4d^9 4f^2 \rightarrow 4d^{10}4f^0 + e^-,$$

where $h\nu$ and e^- stand for an incident photon and a photoelectron, respectively. To interpret the resonant enhancement in CeO_2 using the same arguments, one would have to start from an initial configuration with one electron in the $4f$

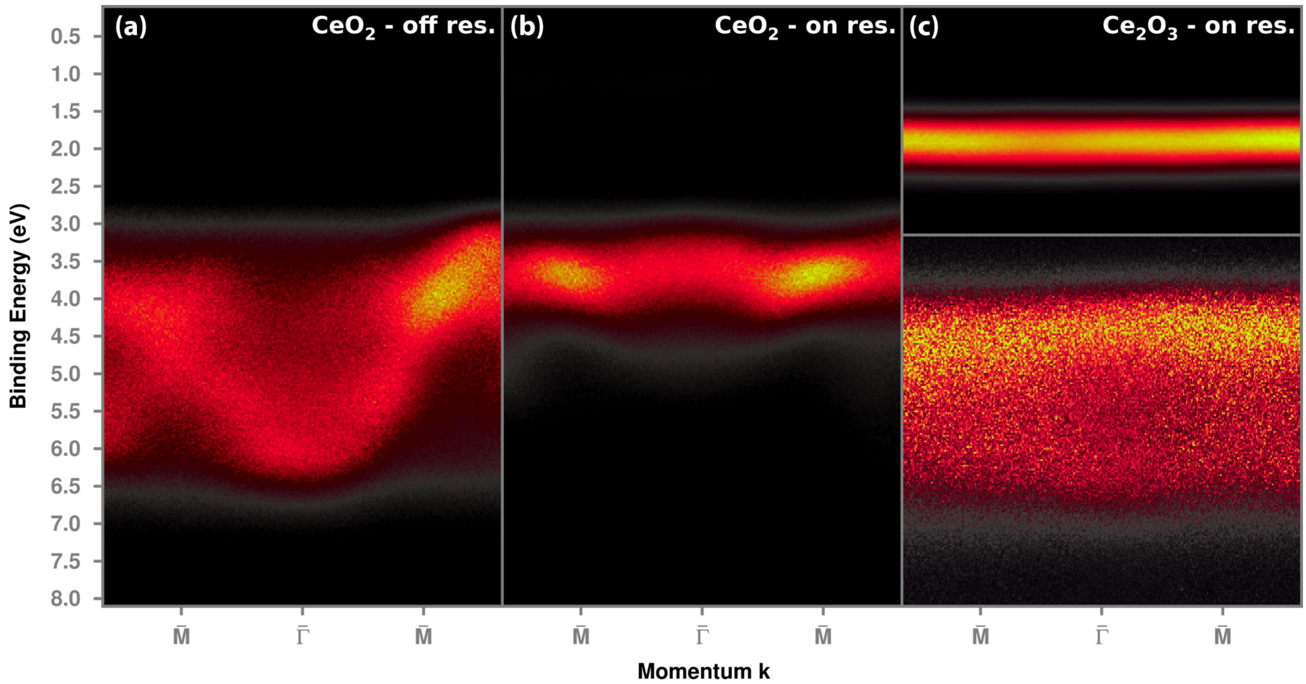

FIG. 2. Dispersion of the valence band in CeO_2 and c–Ce_2O_3 in the $\bar{M}$-$\bar{\Gamma}$-$\bar{M}$ direction of the surface Brillouin zone followed by resonant angle-resolved photoelectron spectroscopy. (a) Valence band of CeO_2 ($h\nu = 115$ eV); (b) and (c) dispersion of the resonant feature at the $4d \rightarrow 4f$ photoabsorption threshold in CeO_2 ($h\nu = 125$ eV) and c–Ce_2O_3 ($h\nu = 121$ eV), respectively. The areas of the energy-dispersive curves were normalized to 1 prior to plotting the maps. The bottom and upper parts of (c) were normalized separately in order to highlight the O $2p$ bands.

level—a $4d^{10}4f^1\,\underline{L}$ state. This would make CeO_2 essentially a $4f^1$ compound in the case of the covalent ground state. Consequently, the assumption of the $4d^{10}4f^1\,\underline{L}$ initial state inevitably leads to the homogeneous mixed valent ground state of CeO_2 with a partial occupation of the $4f$ level through mixing between $4f^0$ and $4f^1\,\underline{L}$ configurations defined by the integer $4f$ occupation number. However, this description is based on the assumed resonant enhancement process at the $4d \rightarrow 4f$ photoabsorption threshold in CeO_2 involving the ground state of the $4f^1\,\underline{L}$ configuration, which is not self-evident. Specifically, the extent of the final-state effects in the resonant photoemission process has not been previously accounted for.

While the occupation of the localized (atomiclike) $4f$ level in the homogeneous mixed valent ground state of ceria is expected to generate a dispersionless photoemission feature, the p-bonding mediated itinerant nature of extended covalent states (of $4f$ and $2p$ symmetry) would give rise to an observable dispersion in ARPES. To examine these effects, we have followed the dispersions at the on-resonance for CeO_2 and c–Ce_2O_3 along the $\bar{M}$-$\bar{\Gamma}$-$\bar{M}$ direction (in surface Brillouin zone notation).

Figures 2(b) and 2(c) show the on-resonance ARPES image plots for CeO_2 and c–Ce_2O_3, respectively. Compared with the off-resonance ARPES image plot for CeO_2 shown in Fig. 2(a), the dispersive features at the binding energy of 3–6 eV are clearly observable. Note that in Fig. 2(b), the Ce $4f$ derived spectral intensity is much enhanced at a binding energy of 3–4 eV where O $2p$ states exist, indicating covalent hybridization between Ce $4f$ and O $2p$. On the other hand, the $4f$ derived spectral feature in c–Ce_2O_3 at a binding energy of 1.9 eV exhibits no discernible dispersion within the experimental resolution [Fig. 2(c)]. These results indicate different resonant photoemission processes in the two compounds: more specifically, there is no occupation of atomiclike localized f states in the ground state of CeO_2.

To further ascertain the covalent hybridization in the valence band of ceria, we have calculated electronic properties in the intermediate states ($4d^94f^1$ for CeO_2 and $4d^94f^2$ for c–Ce_2O_3). The density of states plots are shown in Fig. 1. We find, in agreement with previous DFT studies [36], that the O $2p$ band in the ground state of CeO_2 has a small $4f$ and $5d$ admixture at the top and the bottom of the band, respectively. However, this alone cannot be used to abandon the pure ionic bonding picture in ceria (originating from the nominal electron configuration) as the degree of mixing in the calculated partial density of states is comparable to other recognized ionic compounds, such as NaCl [37]. On the other hand, the intermediate state shows an appreciable increase in the $4f$ admixture into the O $2p$ band, to such an extent that the valence band looks covalent in character. It should be noted that the major increase of the f contribution around 5–6 eV is related to the excited f electron of the intermediate state, which will be further discussed below. This behavior is consistent with closed shell screening of the $4d$ core hole by covalent electrons [38]. Appropriately, the response of O $2p$ electrons to a $4d$ core hole in c–Ce_2O_3 is less significant due to the occupation of the highly localized $4f$ level by two electrons, which can effectively screen the positive charge of the core hole. An interesting aspect of the intermediate $4d^94f^1$

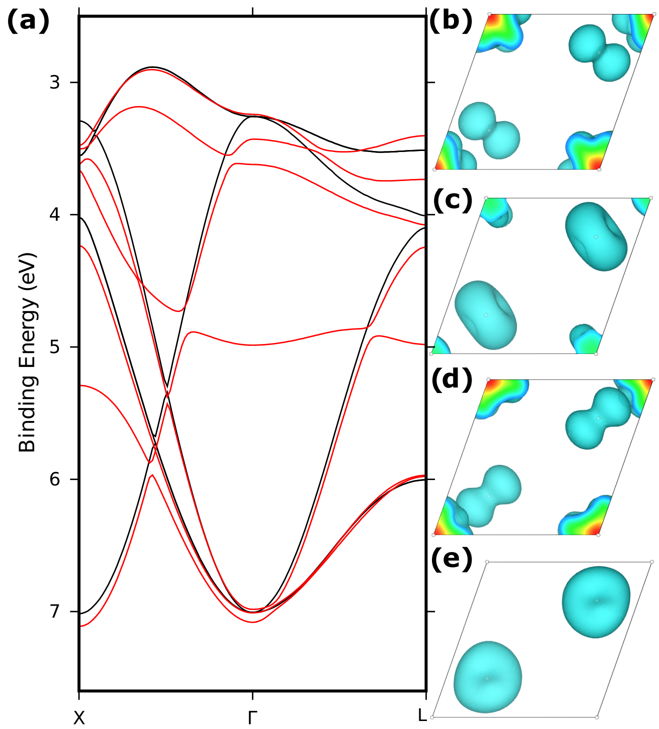

FIG. 3. (a) Band structure of CeO_2 calculated along X-Γ-L for the ground state (black) and the intermediate $4d^9 4f^1$ state (red). The extra $4f^1$ band of the intermediate state is at 5 eV at Γ. The calculated band structure has been shifted by 2.9 eV to coincide with the experimental data. Calculated Kohn-Sham wave functions at the Γ point of CeO_2 in the intermediate state are shown as cyan contours (corresponding to a probability density of 2^{-5}; higher probability densities are shown in warmer colors as visible in cutout areas) in (b) the topmost O $2p$ band, (c) the second O $2p$ band (the third has the same symmetry and is not shown), (d) $4f^1$, and (e) a representation of the bottom three O $2p$ bands. There are four cerium atoms and two oxygen atoms in the corners and in the middle of the displayed cut through the CeO_2 lattice, respectively. Periodic portions of the wave functions have been eliminated for clarity.

state of CeO_2 is that there is no observable gap between the O $2p$ pDOS and the $4f$ pDOS at the Fermi level (Fig. 1).

We examine band-structure calculations along X-Γ-L (in bulk Brillouin zone notation), a straight line close to the experimental setup, for the ground state and the intermediate state of CeO_2 [Fig. 3(a)]. Apart from lifting the degeneracy of the $2p$ bands, it can be seen that as a consequence of the point charge of the core hole, the additional band of the intermediate state appears at 5 eV at Γ, directly overlapping the O $2p$ level. It is noteworthy that the excited electron does not occupy highly localized $4f$ states, but a considerably hybridized one with O $2p$ character.

The enhancement of the spectral intensity at the top of the O $2p$ band [Fig. 2(b)] suggests that the top of the O $2p$ state coupled with the f state plays a major role in the screening response to the core-hole potential. We further rationalize this observation by examining the calculated Kohn-Sham wave functions of the valence bands of the intermediate state of CeO_2. The analysis reveals a distinct difference between the three topmost [Figs. 3(b) and 3(c)] and three bottommost [Fig. 3(e)] O $2p$ bands. While the bottom three bands are localized solely on the O atoms, the three topmost bands are partially localized over the Ce atoms in the intermediate state. The shapes of the orbitals suggest p character on the O atoms and f character on the Ce atoms. The band closest to the Fermi energy has the strongest f character [a minute f character from the band corresponding to Fig. 3(b) has been present on the Ce atoms in the ground state—not shown]. Thus, by participating in the screening of the $4d$ hole on the Ce atom, the top three electrons play a significant role in the Auger decay process of the Ce $4d^9 4f^1$ excited state compared with the rest of the O $2p$ electrons. This is effected by their f character, the proximity in energy, and the wave-function overlap with the $4f^1$ electron [Fig. 3(d)] positively influencing the Coulomb matrix elements, making the Auger decay process with the respective electrons much more probable.

Taking into account the experimental and theoretical findings, the resonant photoemission process in CeO_2, with a $4f^0$ configuration in the ground state and partial covalent bonding character, can be rationalized as a core-level interatomic effect. In contrast to the intra-atomic single-atom resonant photoemission, the electrons participating in the indirect photoemission channel of the resonant process in CeO_2 are primarily associated with two atoms—Ce and O. Specifically, we see an enhancement of the intensity of the photoemission from the top of the O $2p$ band in ceria due to core-level absorption at the $4d \to 4f$ threshold of Ce. This process is known as an intermediate type of multiatom resonant photoemission [39]. We can thus describe the resonant photoemission in CeO_2 as an interference of the following two processes:

$$\begin{aligned}
&(1)\ \ \mathrm{Ce}\,4d^{10}4f^0\ \mathrm{O}\,2p^6 + h\nu \to\ \mathrm{Ce}\,4d^{10}4f^0\ \mathrm{O}\,2p^5 + e^-,\\
&(2)\ \ \mathrm{Ce}\,4d^{10}4f^0\ \mathrm{O}\,2p^6 + h\nu \to\ \mathrm{Ce}\,4d^{9}4f^1\ \mathrm{O}\,2p^6 \to\\
&\qquad\qquad\qquad\qquad\qquad \to\ \mathrm{Ce}\,4d^{10}4f^0\ \mathrm{O}\,2p^5 + e^-.
\end{aligned}$$

Now it is clear that the resonance enhancement at the $4d \to 4f$ threshold for Ce^{4+} and Ce^{3+} atoms is of a profoundly different nature. Since the resonant enhancement of the f derived spectral feature from Ce^{4+} atoms is caused by interatomic effects, it is likely to be sensitive to perturbations such as oxygen vacancies, adsorbates, foreign substitutional and interstitial species, etc. On the other hand, the resonant process for Ce^{3+} atoms is less influenced by the perturbations because it is an intra-atomic transition. This requires reexamination of the widely used formula for derivation of stoichiometry of various ceria-based materials from the ratio of resonant enhancement of Ce^{4+} and Ce^{3+} photoemission [40–44]. Given the widespread use of the method, the observation of the interatomic effects in the resonance photoemission in ceria calls for further study evaluating the validity of the direct proportion between the intensity of the resonant feature and the density of Ce^{4+} atoms with respect to the electronic perturbations in their vicinity.

IV. CONCLUSION

We have presented the results of a combined experimental and theoretical study of the electronic structure of CeO_2. We find that there are no occupied localized f states in the ground state of CeO_2. Instead, we demonstrate that the f contribution in CeO_2 is of a covalent nature, arising from hybridization with the O $2p$ bands. This is in contrast to the nondispersive $4f$ state at 1.9 eV in c–Ce_2O_3, where the O $2p$ bands shift to higher binding energy, reducing mixing with the $4f$ states at the top. We show that, as a consequence of the covalent hybridization, the resonant photoemission process in CeO_2 involves interatomic core-hole screening, which is in contrast to the intra-atomic process in Ce_2O_3. We suggest that the different nature of the two processes should be taken into account when interpreting resonant photoemission experiments from ceria and other covalent materials.

ACKNOWLEDGMENTS

This work was supported by the Czech Science Foundation (GAČR 15-06759S), the Grant Agency of Charles University (GAUK 472216), the Hiroshima Synchrotron Radiation Center (13-B-12), and the Louisiana EPSCoR Program. The computing resources used in the project were provided by LSU-HPC, ORNL, and NERSC. E.F.S acknowledges financial support from the JSPS postdoctoral fellowship for overseas researchers, as well as the Alexander von Humboldt-Stiftung (Grant No. P13783).

[1] A. Fujimori, Phys. Rev. B **28**, 2281 (1983).
[2] D. D. Koelling, A. M. Boring, and J. H. Wood, Solid State Commun. **47**, 227 (1983).
[3] E. Wuilloud, B. Delley, W.-D. Schneider, and Y. Baer, Phys. Rev. Lett. **53**, 202 (1984).
[4] W.-D. Schneider, B. Delley, E. Wuilloud, J.-M. Imer, and Y. Baer, Phys. Rev. B **32**, 6819 (1985).
[5] G. Kaindl, G. K. Wertheim, G. Schmiester, and E. V. Sampathkumaran, Phys. Rev. Lett. **58**, 606 (1987).
[6] F. Marabelli and P. Wachter, Phys. Rev. B **36**, 1238 (1987).
[7] R. C. Karnatak, J.-M. Esteva, H. Dexpert, M. Gasgnier, P. E. Caro, and L. Albert, Phys. Rev. B **36**, 1745 (1987).
[8] M. Matsumoto, K. Soda, K. Ichikawa, S. Tanaka, Y. Taguchi, K. Jouda, O. Aita, Y. Tezuka, and S. Shin, Phys. Rev. B **50**, 11340 (1994).
[9] H. Nakamatsu, T. Mukoyama, and H. Adachi, Chem. Phys. Lett. **247**, 168 (1995).
[10] P. Wachter, Phys. B: Condens. Matter **300**, 105 (2001).
[11] E. Shoko, M. F. Smith, and R. H. McKenzie, Phys. Rev. B **79**, 134108 (2009).
[12] M. B. Robin and P. Day, Adv. Inorg. Chem. Radiochem. **10**, 247 (1968).
[13] P. Day, N. S. Hush, and R. J. H. Clark, Philos. Trans. A Math. Phys. Eng. Sci. **366**, 5 (2008).
[14] L. Pauling, *The Nature of the Chemical Bond and the Structure of Molecules and Crystals: An Introduction to Modern Structural Chemistry* (Cornell University Press, Ithaca, NY, 1960).
[15] C. M. Varma, Rev. Mod. Phys. **48**, 219 (1976).
[16] J.-D. Cafun, K. O. Kvashnina, E. Casals, V. F. Puntes, and P. Glatzel, ACS Nano **7**, 10726 (2013).
[17] D. N. Mueller, M. L. Machala, H. Bluhm, and W. C. Chueh, Nat. Commun. **6**, 6097 (2015).
[18] C. J. Nelin, P. S. Bagus, E. S. Ilton, S. A. Chambers, H. Kuhlenbeck, and H.-J. Freund, Int. J. Quantum Chem. **110**, 2752 (2010).
[19] P. S. Bagus, C. J. Nelin, Y. Al-Salik, E. S. Ilton, and H. Idriss, Surf. Sci. **643**, 142 (2016).
[20] P. S. Bagus and C. J. Nelin, J. Electron Spectrosc. Relat. Phenom. **194**, 37 (2014).
[21] T. Duchoň, F. Dvořák, M. Aulická, V. Stetsovych, M. Vorokhta, D. Mazur, K. Veltruská, T. Skála, J. Mysliveček, I. Matolínová, and V. Matolín, J. Phys. Chem. C **118**, 357 (2014).
[22] V. Stetsovych, F. Pagliuca, F. Dvořák, T. Duchoň, M. Vorokhta, M. Aulická, J. Lachnitt, S. Schernich, I. Matolínová, K. Veltruská, T. Skála, D. Mazur, J. Mysliveček, J. Libuda, and V. Matolín, J. Phys. Chem. Lett. **4**, 866 (2013).
[23] J. Heyd, G. E. Scuseria, and M. Ernzerhof, J. Chem. Phys. **124**, 219906 (2006).
[24] G. Kresse and J. Furthmüller, Phys. Rev. B **54**, 11169 (1996).
[25] G. Kresse and D. Joubert, Phys. Rev. B **59**, 1758 (1999).
[26] L. Gerward, J. Staun Olsen, L. Petit, G. Vaitheeswaran, V. Kanchana, and A. Svane, J. Alloys Compd. **400**, 56 (2005).
[27] P. J. Hay, R. L. Martin, J. Uddin, and G. E. Scuseria, J. Chem. Phys. **125**, 034712 (2006).
[28] G.-y. Adachi and N. Imanaka, Chem. Rev. **98**, 1479 (1998).
[29] A. V. Prokofiev, A. I. Shelykh, and B. T. Melekh, J. Alloys Compd. **242**, 41 (1996).
[30] L. Köhler and G. Kresse, Phys. Rev. B **70**, 165405 (2004).
[31] *Catalysis by Ceria and Related Materials*, edited by A. Trovarelli (Imperial College Press, London, 2002).
[32] M. Zinkevich, D. Djurovic, and F. Aldinger, Solid State Ion. **177**, 989 (2006).
[33] J. L. F. Da Silva, Phys. Rev. B **76**, 193108 (2007).
[34] A. Sekiyama, T. Iwasaki, K. Matsuda, Y. Saitoh, Y. Ônuki, and S. Suga, Nature (London) **403**, 396 (2000).
[35] V. Matolín, M. Cabala, V. Cháb, I. Matolínová, K. C. Prince, M. Škoda, F. Šutara, T. Skála, and K. Veltruská, Surf. Interface Anal. **40**, 225 (2008).
[36] R. Gillen, S. J. Clark, and J. Robertson, Phys. Rev. B **87**, 125116 (2013).
[37] B. Li, A. Michaelides, and M. Scheffler, Phys. Rev. B **76**, 075401 (2007).
[38] P. S. Bagus, E. S. Ilton, and C. J. Nelin, Surf. Sci. Rep. **68**, 273 (2013).
[39] A. W. Kay, F. J. Garcia de Abajo, S.-H. Yang, E. Arenholz, B. S. Mun, N. Mannella, Z. Hussain, M. A. Van Hove, and C. S. Fadley, J. Electron Spectrosc. Relat. Phenom. **114–116**, 1179 (2001).
[40] P. M. Albrecht and D. R. Mullins, Langmuir **29**, 4559 (2013).
[41] Y. Lykhach, S. M. Kozlov, T. Skála, A. Tovt, V. Stetsovych, N. Tsud, F. Dvoák, V. Johánek, A. Neitzel, J. Mysliveček, S. Fabris, V. Matolín, K. M. Neyman, and J. Libuda, Nat. Mater. **15**, 284 (2015).
[42] J. Shi, A. Schaefer, A. Wichmann, M. M. Murshed, T. M. Gesing, A. Wittstock, and M. Bäumer, J. Phys. Chem. C **118**, 29270 (2014).
[43] A. Khare, R. J. Choudhary, K. Bapna, D. M. Phase, and S. P. Sanyal, J. Appl. Phys. **108**, 103712 (2010).
[44] D. C. Grinter, C. Muryn, A. Sala, C.-M. Yim, C. L. Pang, T. O. Menteş, A. Locatelli, and G. Thornton, J. Phys. Chem. C **120**, 11037 (2016).